REVISTA Mundi
Engenharia, Tecnologia e Gestão

INPUT IMPEDANCE OF AN ARTERIAL TREE MODEL

IMPEDÂNCIA DE ENTRADA DE UM MODELO DE ÁRVORE ARTERIAL

Patrícia Fonseca de Brito Anjos[1]

Rodrigo Weber dos Santos[2]

Rafael Alves Bonfim de Queiroz[3]

Abstract: Computational models are used to represent blood flow in large and small arteries and to simulate cardiovascular diseases. Through these models, it is possible to estimate the pressure and blood flow in arterial vessels. However, to reduce the complexity of the model simulation, it is necessary to truncate small arterial domains representing the networks of small arteries and arterioles. At truncation points, the input impedance is used as a boundary condition. This work describes a method based on fractal laws to generate models of arterial trees that represent the truncated arterial districts, and how to calculate the input impedance of these models. The influence of the parameters used in the generation of the arterial tree model on the input impedance is investigated. The results show that the bifurcation exponent and asymmetry ratio most influence the input impedance response of the models.

***Keywords*:** Arterial tree. Input impedance. Hemodynamics.

Resumo: Modelos computacionais são utilizados para representar o escoamento sanguíneo nas grandes e pequenas artérias e simular doenças cardiovasculares. Através destes modelos, é possível estimar a pressão e o fluxo sanguíneo nos vasos arteriais. Entretanto, para reduzir a complexidade da simulação do modelo, é necessário truncar pequenos domínios arteriais representando as redes das pequenas artérias e arteríolas. Nos pontos de truncamento a impedância de entrada é utilizada como condição de contorno. Neste trabalho é descrito um método baseado em leis fractais para gerar modelos de árvores arteriais que representam os distritos arteriais truncados, e como é feito o cálculo da impedância de entrada destes modelos. Investiga-se a influência dos parâmetros utilizados na geração do modelo de árvore arterial na impedância de entrada. Os resultados mostram que o expoente de bifurcação e a razão de simetria foram os que mais influenciaram a resposta de impedância de entrada dos modelos.

***Palavras-chave*:** Árvore arterial. Impedância de entrada. Hemodinâmica.

[1]Doutoranda em Modelagem Computacional, Universidade Federal de Juiz de Fora e patriciafonseca@ice.ufjf.br.
[2]Doutor em Matemática, Universidade Federal de Juiz de Fora e rodrigo.weber@ufjf.edu.br.
[3]Doutor em Modelagem Computacional, Universidade Federal de Juiz de Fora e rafael.bonfim@ice.ufjf.br.

1 INTRODUCTION

Blood pressure profile and blood flow through arterial vessels are essential information for the creation of computational hemodynamic models (DU; HU; CAI, 2015). Through these models, it is possible to study the blood flow and vessel geometry of patients with cardiovascular disease, such as stenosis and aneurysm (TASSO et al., 2018; XU et al., 2018; YU et al., 2018).

In order to reduce the complexity of the blood flow simulation is necessary to truncate small arterial districts, which are downstream arterial trees from the truncation points. At truncation points, a linear relationship between pressure and blood flow is employed as the output boundary condition, called the input impedance (DU; HU; CAI, 2015).

In the literature, one of the computational models used to represent truncated arterial districts is a tree generated based on fractal laws (COUSINS; GREMAUD, 2012; DUANMU et al., 2019; OLUFSEN, 1998; STEELE; OLUFSEN; TAYLOR, 2007; XU et al., 2018). According to (OLUFSEN, 1998), the model reproduces characteristics of the pulse wave in hemodynamic simulations.

The objective of this work is to calculate the input impedance of arterial tree models and to investigate the impact of the parameters of these models in the impedance response. Therefore, the methods used were developed by (OLUFSEN et al., 2000), and the parameters adopted in numerical experiments were taken from (COUSINS; GREMAUD, 2012).

The work is organized as follows. Section 2 describes the method of generating arterial trees based on fractal laws. Section 3 depicts the mathematical modeling of the input impedance. Section 4 shows the results of the simulations, and Section 5, the conclusions of the research and future work.

2 GENERATION OF ARTERIAL TREE MODEL

The models are generated based on fractal laws. In the literature, arterial tree models generated from this method are also known as structured tree models. Arterial model trees are generated by a method based on the assumptions listed below (OLUFSEN, 1998; OLUFSEN et al., 2000):

- the arterial tree is modeled as a dichotomously branching (binary) system. The bifurcations are created from the root segment (vessel) of the tree, which has radius r_{iroot} (constant);
- the arterial tree is branched until all terminal segments have a radius of less than a

minimum radius r_{min} given at the start of the simulation;

- the relationship between the radius of the parent segment (r_i) and the radius of daughter segments (r_{dl} and r_{dr}) at each bifurcation satisfies the power law:

$$r_i^{\gamma} = r_{dl}^{\gamma} + r_{dr}^{\gamma}, \tag{1}$$

where r_{dl} is the radius of the daughter segment to the left of the bifurcation, r_{dr} is the radius of the daughter segment to the right, and γ is the exponent of the bifurcation. The coefficient γ is kept constant throughout the tree generation and its value is an input data from the algorithm;

- the asymmetry of the segments is characterized from the area ratio (η) and asymmetry ratio (σ), which are defined by

$$\eta = \frac{r_{dl}^2 + r_{dr}^2}{r_i^2} \tag{2}$$

and

$$\sigma = \left(\frac{r_{dr}}{r_{dl}}\right)^2; \tag{3}$$

- the parameters γ, η and σ are independent, but it is possible to obtain a relationship between them given by:

$$\eta = \frac{1+\sigma}{(1+\sigma^{\frac{\gamma}{2}})^{\frac{2}{\gamma}}}; \tag{4}$$

- in addition to the power law (Eq. 1), there is the following relation in each bifurcation created to scale the tree radii:

$$\begin{aligned} r_{dl} &= \alpha r_i, \\ r_{dr} &= \beta r_i, \end{aligned} \tag{5}$$

where the parameters α and β are obtained from the coefficients γ and σ, through the equations below:

$$\begin{aligned} \alpha &= (1+\sigma^{\frac{\gamma}{2}})^{-1/\gamma}, \\ \beta &= \alpha\sqrt{\sigma}; \end{aligned} \tag{6}$$

- the length of each segment (l_i) is given by

$$l_i = r_i l_{rr}, \tag{7}$$

where l_{rr} is the radius relation that is constant during the simulation. In the literature, there are works reporting that l_{rr} varies depending on the arterial tree model created,

based on the organ where that tree will supply blood (MALVE et al., 2014; STEELE; OLUFSEN; TAYLOR, 2007) . In (IBERALL, 1967; OLUFSEN, 1998), it is reported that a good choice for small arteries is $l_{rr} = 50$.

The Algorithm 1 describes the steps for generating of arterial tree model. The input data of the algorithm are: the root radius r_{iroot}, the minimum radius r_{min}, the length to radius relation l_{rr}, the bifurcation exponent γ and the asymmetry ratio σ. A segment of the tree model has radius r_i, length l_i, and can have daughters on the left (dl) and on the right (dr). The algorithm is recursive. The first segment created in the tree is its root and its daughters on the left and right (lines 6 and 7). $GenerateTree(r_{iroot}, r_{min}, l_{rr}, \gamma, \sigma)$ denotes an algorithm call. If the radius of segment i is greater than or equal to r_{min}, then the daughters of this segment are created (lines 13 and 14). Segments are generated until all terminal segments have radius less than r_{min}.

Algorithm 1: GenerateTree(r_i, r_{min}, l_{rr}, γ, σ).

```
1  if the tree has no segments then
2      r_i = r_iroot;
3      l_i = r_iroot l_rr;
4      α = (1 + σ^(γ/2))^(-1/γ);
5      β = α√σ;
6      Create the daughter to left of segment iroot: r_dl = α r_iroot and l_dl = r_dl l_rr;
7      Create the daughter to right of segment iroot: r_dr = β r_iroot and l_dr = r_dr l_rr;
8      if r_dl ≥ r_min then
9          GenerateTree(r_dl, r_min, l_rr, γ, σ);
10     if r_dr ≥ r_min then
11         GenerateTree(r_dr, r_min, l_rr, γ, σ);
12 else
13     Create the daughter to left of segment i: r_dl = α r_i and l_dl = r_dl l_rr;
14     Create the daughter to right of segment i: r_dr = β r_i and l_dr = r_dr l_rr;
15     if r_dl ≥ r_min then
16         GenerateTree(r_dl, r_min, l_rr, γ, σ);
17     if r_dr ≥ r_min then
18         GenerateTree(r_dr, r_min, l_rr, γ, σ).
```

3 CALCULATION OF INPUT IMPEDANCE

The input impedance of the arterial tree model at the proximal position of the root segment is defined by (OLUFSEN et al., 2000):

$$Z(x, \omega) = \frac{P(x, \omega)}{Q(x, \omega)}, \tag{8}$$

DOI: 10.21575/25254782rmetg2020vol5n21176

where P is pressure and Q is flow in Fourier's space, x is a position of segment where this property is calculated, and ω is the angular frequency.

In (OLUFSEN et al., 2000) it is described a method to obtain the impedance of the models from Navier-Stokes equations. The blood is assumed incompressible fluid, in laminar flow, and neglect the effects of gravity. These equations are linearized, and from the solution of the continuity and momentum equations for the small arteries, it is possible to obtain the pressure and the flow. These parameters are periodic and represented in Fourier's space (OLUFSEN et al., 2000; QURESHI et al., 2014). The following shows how to obtain a mathematical expression for input impedance based on (OLUFSEN, 1998; OLUFSEN et al., 2000).

The continuity and momentum equations are respectively given by (OLUFSEN et al., 2000):

$$j\omega CP + \frac{\partial Q}{\partial x} = 0, \tag{9}$$

$$j\omega Q + \frac{A_i(1-F)}{\rho}\frac{\partial P}{\partial x} = 0, \tag{10}$$

where A_i is the the cross-sectional area of segment i, ρ is the density of fluid and j the imaginary unit and

$$F = \frac{2J_1(w_0)}{w_0 J_0(w_0)}, \tag{11}$$

where J_0 and J_1 are the zeroth and first order Bessel functions, respectively, $w_0 = \sqrt{j^3 w^2}$, $w^2 = r_i^2\omega/\nu$ is the Womersley number, and ν is the kinematic viscosity (ratio between viscosity and density $\nu = \mu/\rho$). F is approximated by (OLUFSEN, 1998):

$$F = \begin{cases} 2/(wj^{1/2})[1 + (2w)^{-1}], & \text{for } w > 3, \\ (3-w)[1 - j(w^2/8) - (w^4/48)] + (w-2)\{2/(wj^{1/2})[1 + (2w)^{-1}]\}, & \text{for } 2 < w \leq 3, \\ 1 - j(w^2/8) - (w^4/48), & \text{for } w \leq 2. \end{cases} \tag{12}$$

In Eq. (9), the parameter C is the compliance of vessel defined by:

$$C = \frac{3A_i r_i}{2Eh}. \tag{13}$$

In order to calculate the compliance we use a relationship between the Young's modulus (E), the wall thickness (h) and the radius (r_i):

$$\frac{Eh}{r_i} = k_1 \exp(k_2 r_i) + k_3, \tag{14}$$

where $k_1 = 2.0 \times 10^7\ g/(s^2 cm)$, $k_2 = -22.53\ cm^{-1}$ and $k_3 = 8.65 \times 10^5\ g/(s^2 cm)$ are

constants (COUSINS; GREMAUD, 2012).

Differentiating Eq. (9) with respect to x, and inserting the result in (10) gives

$$\frac{\omega^2}{c^2}Q + \frac{\partial^2 Q}{\partial x^2} = 0, \tag{15}$$

where c is the wave-propagation velocity (OLUFSEN et al., 2000):

$$c = \sqrt{\frac{A_i(1-F)}{\rho C}}. \tag{16}$$

Solving (15) and inserting in (9) gives

$$Q(x,\omega) = a\cos(\omega x/c) + b\sin(\omega x/c) \tag{17}$$

and

$$P(x,\omega) = j\sqrt{\frac{\rho}{CA_i(1-F)}}\left(-a\sin(\omega x/c) + b\cos(\omega x/c)\right), \tag{18}$$

where a and b are arbitrary constants of integration. Replace the above result in Eq. (8), gives

$$Z(x,\omega) = \frac{jg^{-1}(b\cos(\omega x/c) - a\sin(\omega x/c))}{a\cos(\omega x/c) + b\sin(\omega x/c)}, \tag{19}$$

where

$$g = \sqrt{\frac{CA_i(1-F)}{\rho}}. \tag{20}$$

When Eq. (19) is evaluated at the point $x = l_i$, that is, at the distal point of the vessel, obtains

$$Z(l_i,\omega) = \frac{jg^{-1}(b\cos(\omega l_i/c) - a\sin(\omega l_i/c))}{a\cos(\omega l_i/c) + b\sin(\omega l_i/c)}, \tag{21}$$

and when it is evaluated at the proximal point ($x = 0$),

$$Z(0,\omega) = \frac{jb}{ga}. \tag{22}$$

Assuming $Z(l_i,\omega)$ is known, it is possible to find b/a using Eq. (21) and doing some algebraic manipulations (OLUFSEN, 1998). Thus, the input impedance is given by:

$$Z(0,\omega) = \frac{jg^{-1}\sin(\frac{\omega l_i}{c}) + Z(l_i,\omega)\cos(\frac{\omega l_i}{c})}{\cos(\frac{\omega l_i}{c}) + jgZ(l_i,\omega)\sin(\frac{\omega l_i}{c})}. \tag{23}$$

For any segment, the input impedance when $\omega = 0$ can be found from

$$Z(0,0) = \lim_{\omega \to 0} Z(0,\omega) = \frac{8\mu l_i}{\pi r_i^4} + Z(l_i, 0). \tag{24}$$

In order to compute Eqs. (9) and (10) it is necessary to establish outflow boundary conditions and bifurcation conditions.

In the bifurcation, we assume that is analogous to a transmission-line network

$$\frac{1}{Z_p(l_i,\omega)} = \frac{1}{Z_{dl}(0,\omega)} + \frac{1}{Z_{dr}(0,\omega)}. \tag{25}$$

The condition imposed in terminal segments is the impedance is zero, that is

$$Z_{term}(l_i, \omega) = 0. \tag{26}$$

The algorithm receives as input data to calculate the impedance: the arterial tree model with its segments characterized by its radii and lengths, the angular frequency ω_k, the density ρ and the viscosity μ of blood.

Assume T as the period and N the number of time steps. The impedance should be determined for all discrete angular frequencies $\omega_k = 2\pi k/T$, for $k = 0, \ldots, N$.

The Algorithm 2 calculates the impedance for a frequency of w_k recursively. As the objective is to calculate the input impedance of the tree, for each ω_k, the algorithm is called passing the root segment of the tree (seg_{iroot}) as input data. In the algorithm, Z_{li} refers to the

impedance at the distal point of the i segment, previously denoted by $Z(l_i, \omega)$.

Algorithm 2: $Z(seg_i, \omega_k, \mu, \rho)$.

if $\mathbf{x}_i$ *is the terminal segment* **then**
    $Z_{li} = 0$;
else
    Calculate the impedance of the daughter segment to the left of i: $Z_{dl} = Z(seg_{idl}, \omega_k, \mu, \rho)$;
    Calculate the impedance of the daughter segment to the right of i: $Z_{dr} = Z(seg_{idr}, \omega_k, \mu, \rho)$;
    $Z_{li} = 1/[Z_{dl}^{-1} + Z_{dr}^{-1}]$;
if $\omega_k = 0$ **then**
    Z_i is computed using Eq. (24);
else
    Calculate the parameters: F (see Eq. (12)), C (Eq. (13)), c (Eq. (16)) and g (Eq. (20));
    Z_i is computed using Eq. (23).
Return Z_i.

4 RESULTS

In this section, the results obtained with Algorithms 1 and 2 are presented. These algorithms were implemented in C language.

To validate the implementation, results of simulation are compared with those obtained by (COUSINS; GREMAUD, 2012). We used the following parameters in the generation of the arterial tree model and to calculate the impedance (COUSINS; GREMAUD, 2012): bifurcation exponent $\gamma = 2.76$, asymmetry ratio $\sigma = 0.41$, root radius $r_{iroot} = 0.2\ cm$, minimum radius $r_{min} = 0.007\ cm$, length to radius relation $l_{rr} = 50$. Impedance was calculated using the following input data: density $\rho = 1.06\ gcm^{-3}$ and viscosity $\mu = 0.0488\ gcm^{-1}s^{-1}$. The results are shown in Figure 1.

From Figure 1, the result obtained in this work is in accordance with the numerical data by (COUSINS; GREMAUD, 2012). According to Nichols, et al. (2011), this is the expected behavior for the input impedance module, as a typical impedance module starts with high resistance, since its maximum is reached when the frequency is zero, and then decreases quickly before vary at higher frequencies.

In this work, we also investigated the influence of the parameters of the generation of the arterial tree model in the input impedance value. The parameters considered in this study were: minimum radius r_{min}, bifurcation exponent γ, asymmetry ratio of the segments σ and length to radius relation l_{rr}. A similar study was done by (OLUFSEN, 1998).

Figure 2 shows the input impedance module for models generated with $r_{min} = 0.004, 0.006, 0.008$ and 0.01. It is observed that the parameter interfered in the values of the module of the input impedance. A greater difference can be seen for lower frequencies. Figure 3 shows that decreasing the minimum radius (r_{min}) implies an increase in the root input impedance when ω is equal to zero. The same was observed in (OLUFSEN, 1998).

Figure 4 displays the input impedance module for models with bifurcation exponent $\gamma = 2.3, 2.5, 2.7$ and 2.8. The impedance of the models with bifurcation exponent 2.3 and 2.5 presented more oscillations in the higher frequencies. The Figure 5 shows the input impedance decreases when the bifurcation exponent γ increases.

Figure 6 shows the module of the input impedance when models were generated with different length to radius relation $l_{rr} = 40, 50, 70$ and 80. The root impedance considering the frequency $\omega = 0$ increases as the length to radius relation l_{rr} increases. This makes sense since when changing this value, there is a change in the entire structure of the tree, more specifically in the length of the segments, thus, it ends up altering the propagation characteristics of the wave (OLUFSEN, 1998). The models studied in this work consider the vessels as cylindrical tubes. It is known from the study of flow in tubes that long, thin tubes produce greater resistance than short, thick tubes. This fact explains the linear growth of the root impedance $Z(0, 0)$ shown in Figure 7. This result was also observed in (OLUFSEN, 1998).

Figure 8 shows the results of the input impedance module for tree models with asymmetry ratio $\sigma = 0.3, 0.4, 0.6$ and 0.7. It is observed that the variations in the impedance module for low frequencies increase when σ gets closer to 1. As in the variation of the bifurcation exponent, here, there was also a decrease in the input impedance of the model, $Z(0, 0)$ as the asymmetry ratio σ between the segments increase (Figure 9).

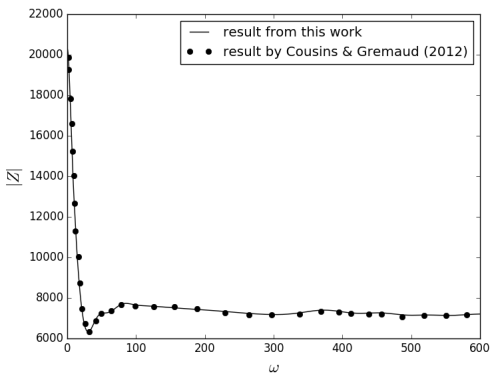

Figure 1: The input impedance module obtained with Algorithm 2.

DOI: 10.21575/25254782rmetg2020vol5n21176

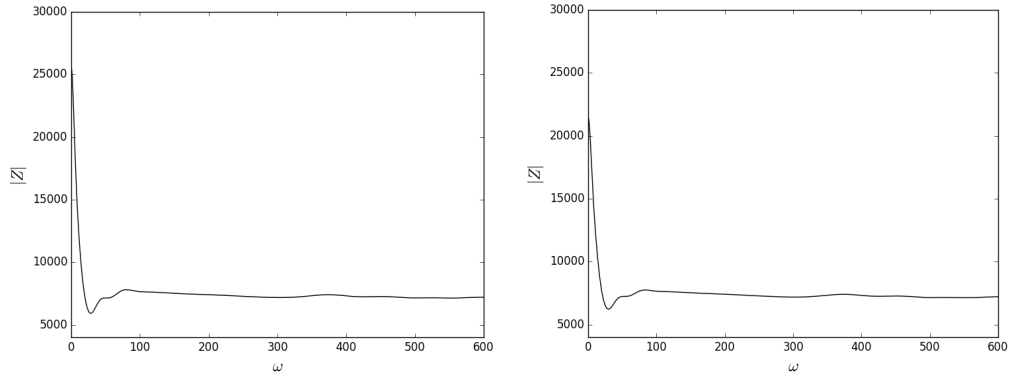

(a) $r_{min} = 0.004$ (b) $r_{min} = 0.006$

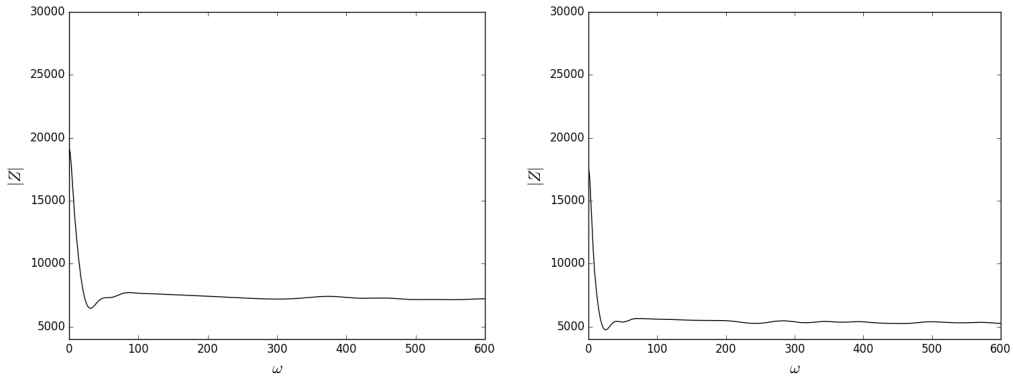

(c) $r_{min} = 0.008$ (d) $r_{min} = 0.01$

Figure 2: The input impedance module for $r_{min} = 0.004, 0.006, 0.008$ and 0.01.

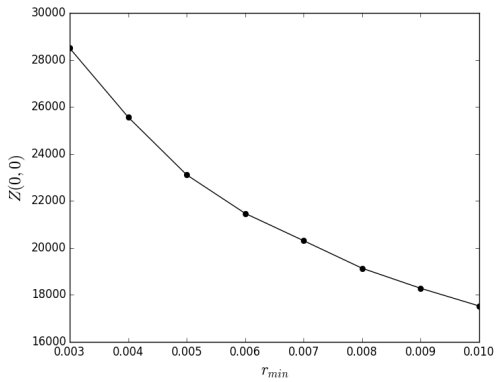

Figure 3: $Z(0, 0)$ as a function of minimum radius r_{min}.

DOI: 10.21575/25254782rmetg2020vol5n21176

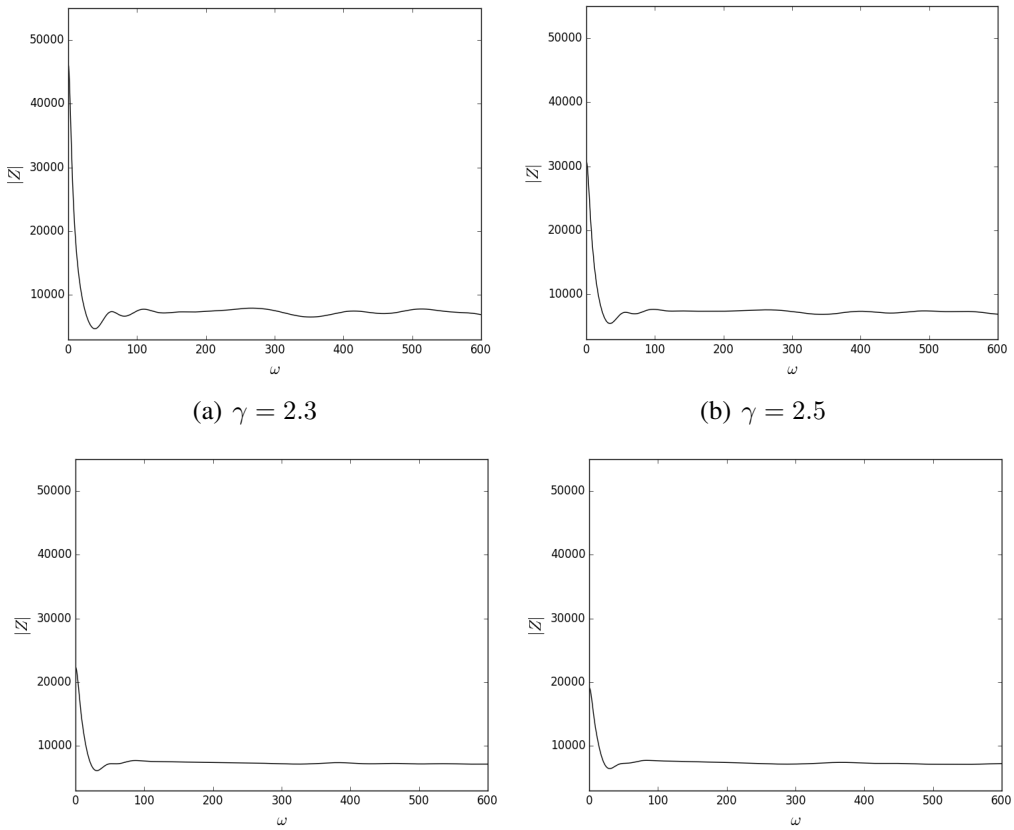

(a) $\gamma = 2.3$ (b) $\gamma = 2.5$

(c) $\gamma = 2.7$ (d) $\gamma = 2.8$

Figure 4: The input impedance module for $\gamma = 2.3$, 2.5, 2.7 and 2.8.

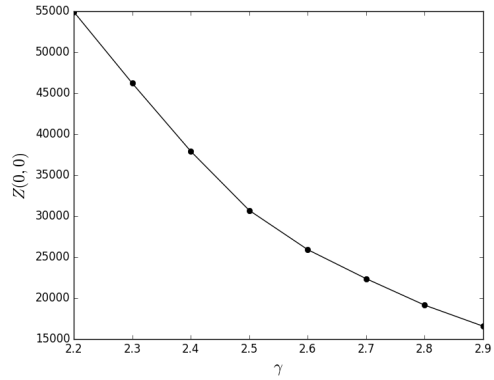

Figure 5: $Z(0,0)$ as a function of bifurcation exponent γ.

DOI: 10.21575/25254782rmetg2020vol5n21176

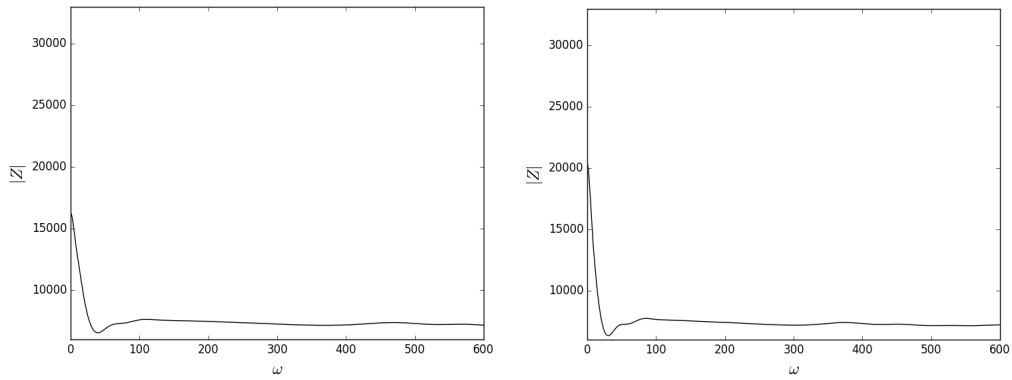

(a) $l_{rr} = 40$ (b) $l_{rr} = 50$

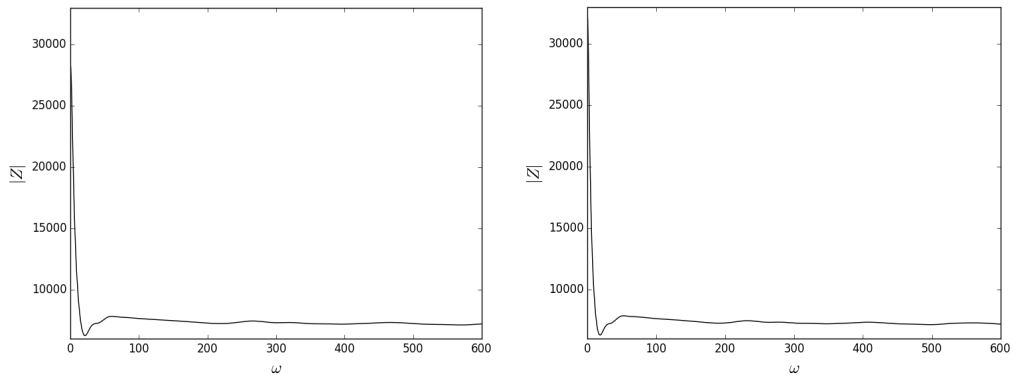

(c) $l_{rr} = 70$ (d) $l_{rr} = 80$

Figure 6: The input impedance module for $l_{rr} = 40$, 50, 70 and 80.

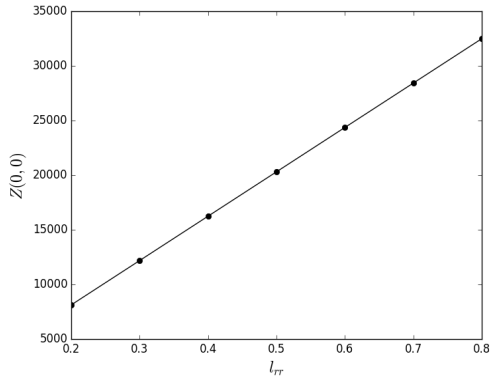

Figure 7: $Z(0, 0)$ as a function of length to radius relation l_{rr}.

DOI: 10.21575/25254782rmetg2020vol5n21176

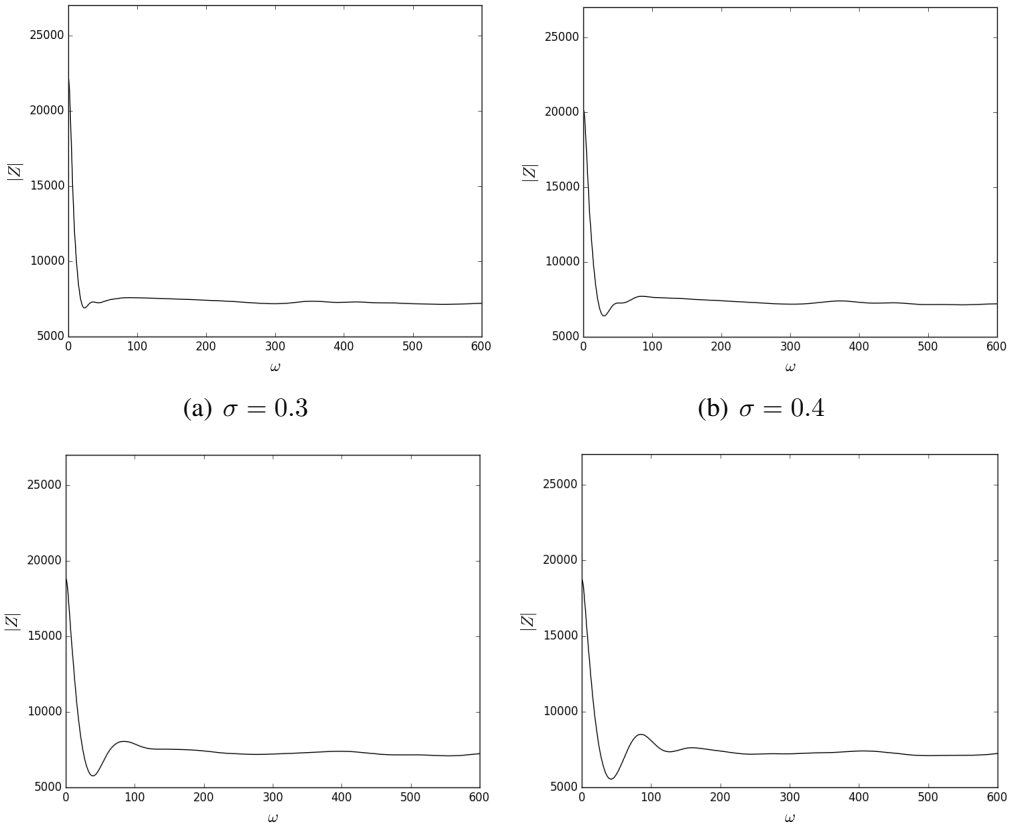

(a) $\sigma = 0.3$ (b) $\sigma = 0.4$

(c) $\sigma = 0.6$ (d) $\sigma = 0.7$

Figure 8: The input impedance module for $\sigma = 0.3$, 0.4, 0.6 and 0.7.

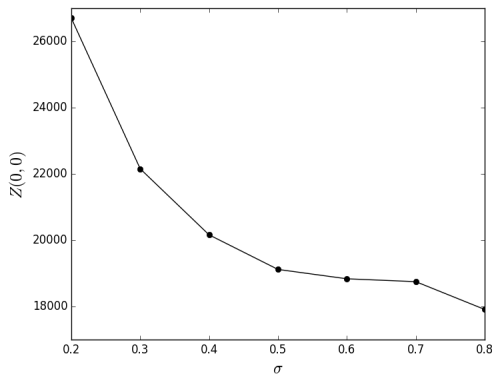

Figure 9: $Z(0, 0)$ as a function the asymmetry ratio σ.

5 CONCLUSIONS

This work presented a new method that generates arterial tree models based on fractal laws and how the input impedance of these models can be calculated.

From these arterial tree models, it is possible to obtain an input impedance whose behavior of the curve of the module is consistent with experiments made *in vivo* (NICHOLS; O'ROURKE; VLACHOPOULOS, 2011). In addition, this work shows that the choice of parameters for model generation influences the characterization of the input impedance.

As future work, we intend to study the blood flow in the arterial system using this input impedance as an output boundary condition, and also to use other methods to generate arterial tree models.

ACKNOWLEDGMENTS

The authors acknowledges the support from Coordenação de Aperfeiçoamento de Pessoal de Nível Superior - Brasil (CAPES) - Finance Code 001, Fundação de Amparo à Pesquisa do Estado de Minas Gerais (FAPEMIG) and INCT-MACC (Instituto Nacional de Ciência e Tecnologia - Medicina Assistida por Computação Científica), approved form CNPq.

REFERENCES

COUSINS, W.; GREMAUD, P. A. Boundary conditions for hemodynamics: the structured tree revisited. *Journal of Computational Physics*, v. 231, p. 6086–6096, 2012.

DU, T.; HU, D.; CAI, D. Outflow boundary conditions for blood flow in arterial trees. *Plos One*, v. 10, 2015.

DUANMU, Z. et al. A one-dimensional hemodynamic model of the coronary arterial tree. *Frontiers in Physiology*, v. 10, 2019.

IBERALL, A. S. Anatomy and steady flow characteristics of the arterial system with an introduction to its pulsatile characteristics. *Mathematical Biosciences*, v. 1, p. 375–395, 1967.

MALVE, M. et al. Impedance-based outflow boundary conditions for human carotid haemodynamics. *Computer Methods in Biomechanics and Biomedical Engineering*, v. 17, n. 11, p. 1248–1260, 2014.

NICHOLS, W. W.; O'ROURKE, M. F.; VLACHOPOULOS, C. *McDonald's Blood Flow in Arteries, Theoretical, Experimental and Clinical Principles*. 6ª. [S.l.]: Hodder Arnold, 2011.

OLUFSEN, M. S. *Modeling the arterial system with reference to an anesthesia simulator*. Tese (Doutorado) — Roskilde University, Roskilde, Denmark, 1998.

OLUFSEN, M. S. et al. Numerical simulation and experimental validation of blood flow in arteries with structured-tree outflow conditions. *Annals of Biomedical Engineering*, v. 28, p. 1281–1299, 2000.

QURESHI, M. U. et al. Numerical simulation of blood flow and pressure drop in the pulmonary arterial and venous circulation. *Biomechanics and Modeling in Mechanobiology*, v. 13, p. 1137–1154, 2014.

STEELE, B. N.; OLUFSEN, M. S.; TAYLOR, C. A. Fractal network model for simulating abdominal and lower extremity blood flow during resting and exercise conditions. *Computer Methods in Biomechanics and Biomedical Engineering*, v. 10, p. 39–51, 2007.

TASSO, P. et al. Abdominal aortic aneurysm endovascular repair: profiling postimplantation morphometry and hemodynamics with image-based computational fluid dynamics. *Journal of Biomechanical Engineering*, v. 140, 2018.

XU, P. et al. Assessment of boundary conditions for CFD simulation in human carotid artery. *Biomechanics and Modeling in Mechanobiology*, p. 1–17, 2018.

YU, H. et al. A multiscale computational modeling for cerebral blood flow with aneurysms and/or stenoses. *International Journal for Numerical Methods in Biomedical Engineering*, 2018.

Edição especial - XXII ENMC (Encontro Nacional de Modelagem Computacional) e X ECTM (Encontro de Ciência e Tecnologia dos Materiais)

Enviado em: 02 abr. 2020

Aceito em: 13 mai. 2020

Editor responsável: Rafael Alves Bonfim de Queiroz